Modelling of Fatigue in Some Steels and Non-Ferrous Alloys

Donka Angelova, Rozina Yordanova
University of Chemical Technology and Metallurgy-Sofia,
8 Kl. Ohridski Blvd., 1756 Sofia, Bulgaria
donkaangelova@abv.bg, rozi.yordanova@abv.bg

Key words: fatigue, short fatigue-crack, modelling, law-carbon steel, copper, Ti-alloy

Abstract. For most engineering alloys the plot of short fatigue crack growth rate against crack length can be modeled by parabolic-linear system of equations. This model is illustrated on two low-carbon steels subjected to tension-tension loading. At elastic-plastic fracture mechanics conditions, the fatigue-data presentation including short fatigue crack growth rate against J-integral range takes place for some steels and non-ferrous alloys based on titanium and copper.

An alternative method of short fatigue crack data presentation is proposed that involves a specific energy fatigue-function expressed by an almost straight line termed *fatigue tendency* of the material at a given stress-range. A comparative analysis between the standard and new presentations shows that at the same number of crack-size measurements, the precision of the latter is significantly higher.

This result suggests a possible decrease of fatigue measurements and is approved for another 20 materials.

Introduction

Although major advances have been made in fatigue modelling, the application of fatigue concepts to different practical situations is highly individual and often involves empirical and semi-empirical approaches including a large number of specifying constants. In linear elastic fracture mechanics one of the most used presentations "Long fatigue crack growth rate, da_l / dN against Stress-intensity factor range ΔK_l" includes, in log-log scales, three regimes of crack growth, [1]: **I,** of threshold development; **II,** of Paris linear propagation, $\log(da_l / dN) = C(\log \Delta K)^m$, where a_l is long fatigue-crack size, N – number of cycles, C and m – scaling constants; and **III,** of rapid increase of da_l / dN leading to the final failure. The micro-approach of short fatigue crack propagation presents plot "Fatigue crack growth rate da_{sh} / dN against Crack length a_{sh}" on log-log scales that consists of two regimes corresponding to so called small and long crack stages revealed by Brown and Hobson [2], and in more precise terms – of three regimes introduced by Angelova and Akid [3]: **I** of short crack growth, mode II; **II** of physically small crack growth, mode I; and **III** of long crack growth. A similar three regimes presentation with different mathematical description is offered by Yordanova [4]. The first regime of Brown-Hobson model and the first two regimes of Angelova-Akid and Yordanova models are described by parabolas and the final regime in all of them – by lines. Sometimes the obtained short fatigue crack data can be represent in the same way that is used for the long fatigue crack data presentation, namely: "Short fatigue crack growth rate, da_{sh} / dN against Short fatigue crack equivalent to ΔK_l, $\Delta K_{sh} = k\sigma\sqrt{a_{sh}}$" or $\log da_{sh} / dN - \log \Delta K_{sh}$, Gangloff [5]. At elastic-plastic fracture mechanics conditions, a presentation "Short fatigue crack growth rate da_{sh} / dN against J-integral range, ΔJ" or $\log da_{sh} / dN - \log \Delta J$ takes place for some steels and nonferrous alloys as it is shown in Hoshide [6, 7] and Dowling [8]. A new mechanism of fatigue failure at inclusion presence in ultralong life regime, when N>107 cycles, has been investigated,

described and supplied with an efficient model for practical uses by Murakami [9]. This model is based on the parameter of a specific optically dark area (ODA) introduced in 2000 by Murakami that plays a critical role for the ultralong fatigue conditions.

In the present study, conventional fatigue models presented by that of Yordanova and an alternative method for fatigue data presentation are proposed. The alternative method comprises more precise fatigue testing of engineering materials and a specific presentation of fatigue crack growth data, based on an energy fatigue-function ΔW introduced by Angelova [10, 11] in its different versions – $\Delta W = (da/dN)\Delta K$, $kW = k(da/dN)\Delta K$), $\Delta W = (da/dN)\Delta J$, $\Delta W = \Delta\sigma(da/dN)a^{1/2}$.

Experimental Procedure

Two low-carbon steels were under our investigations. A low-carbon roller-quenched tempered steel, RQT501, used for offshore applications was subjected to tension-tension loading at a stress ratio R = 0.1 using a servo-electric fatigue rig with a load capacity of 100kN. Tests were performed in load control at stress levels of 396MPa, 470MPa and 516MPa within a 0.6M *NaCl* environment [3]. A sinusoidal waveform was used at frequencies 0.2Hz, 0.5Hz and 1Hz. A low-alloyed construction steel, ROLCLAS-09G2, also used for offshore applications was subjected to tension-tension loading at the same stress ratio R = 0.1. Tests were carried out on fatigue machine Amsler under stress ranges 387MPa, 396Mpa, 405Mpa and at frequency 190Hz. The chemical composition and mechanical characteristics of both steels are shown in Table 1.

Chemical Composition, wt %												
Steels	**C**	**Si**	**Mn**	**Cr**	**Ni**	**P**	**S**	**Cu**	**Al**	**As**	**Mo**	**V**
ROLCLAS-09G2	0.09	0.28	1.63	0.05	0.04	0.017	0.026	0.13	0.12	0.014	–	–
RQT501	0.12	0.30	1.45	0.02	0.02	0.011	0.003	0.02	0.045	–	0.01	0.01

Mechanical Properties				
Steels	**Tensile Strength σ_B [MPa]**	**Proof strength $\sigma_{0.2}$ [MPa]**	**Elongation %**	**Average grain size [μm]**
ROLCLAS-09G2	475.3	382.2	28	25
RQT501	608	508	22	8.6

Table 1. Steels characteristics

Pit and short crack initiation and growth were monitored by surface replication of smooth hourglass specimen, Fig. 1, and their diameters and lengths – measured with the help of an image-analysis system.

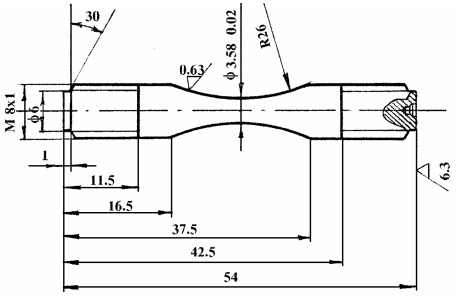

Figure1 Shape of steel specimen. (Dimensions are in *mm*)

The present study considers as well the elastic-plastic fatigue behavior of two non-ferrous alloys investigated by Hoshide [6, 7]. One of them is a heat treated rolled Ti-6Al-4V titanium alloy,

$(\alpha+\beta)$Ti alloy, subjected to fully-reversed axial and combined axial-torsional fatigue loading at frequency of 0.8Hz and stress levels 2200MPa, 2000MPa, 1800MPa; the test specimens are shown in Fig. 2–***a***, [6]. The other alloy is oxygen-free high-conductivity (OFHC) copper exposed to fully-reversed push-pull low-cycle loading of displacement controlled condition in a close loop servo-hydraulic testing rig.

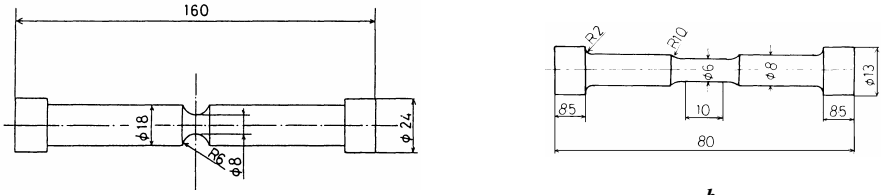

a. ***b.***

Figure 2. Shape of different fatigue specimens used by Hoshide, [6, 7]:
(*a*) Circumferential notched specimen for $(\alpha+\beta)$ Ti alloy;
(*b*) Complicated cylindrical-shaped specimen for OFHC copper. (Dimensions are in *mm*)

Test strain ranges are $\Delta\varepsilon = 0.49\%, 0.68\%, 0.91\%$; The different-alloy specimens can be shown in Fig. 2–***b***, [7]. The most important characteristics of both alloys are presented in Table 2 [6, 7].

Chemical Composition, wt %				
Non-Ferrous Alloys	**Al**	**V**	**Fe**	**O**
$(\alpha+\beta)$**Ti Alloy**	6.52	4.00	0.16	0.182
OFHC Copper	Oxygen-free high conductivity copper with 99% purity and 3 ppm oxygen			

Mechanical Properties						
Non-Ferrous Alloys	**Heat Treatment**	**Tensile Strength σ_B [MPa]**	**0.2% Proof Strength; Yield Strength σ_y [MPa]**	**Young Modulus [GPa]**	**Elongation [%]**	**Average grain size [μm]**
$(\alpha+\beta)$**Ti Alloy**	After the $(\alpha+\beta)$ rolling the alloy was annealed at 1023 K for 2hr in ambient atmosphere, followed by air cooling	994	913	110	18,8	α -grain 8.5
OFHC	Annealed at 600°C for 1hr in vacuum and cooled in furnace	216	40.6	122	80.0	97

Table 2. Non-ferrous alloys characteristics

The behaviour of short fatigue cracks in both non-ferrous alloys is observed by employing a plastic replication technique. In the case of OFHC copper long through-thickness cracks have been used as well. Thus, the growth rate of short cracks in OFHC copper has been correlated to ΔJ -range and this relation – compared with the ΔJ presentation of long through-thickness crack growth.

Results, analyses and discussion

The three distinct regimes $da/dN - a$ describing the fatigue behaviour of RQT501 and ROLCLAS-09G2 – those of microstructurally short fatigue cracks a_{sh}, SFC; physically small fatigue cracks a_{phs}, PSFC; and long fatigue cracks a_l, LFC – were modelled by parabolic-linear system of equations M, shown in Eqs. (1):

$$\mathbf{M(a):}\begin{cases} SFC:\left(\frac{da}{dN}\right)_{sh} = A_1a^2 + A_2a + A_3;\ a \in [a_0,\ d_1] \\ PSFC:\left(\frac{da}{dN}\right)_{phs} = B_1a^2 + B_2a + B_3;\ a \in [d_1,\ d_2] \\ LCF:\left(\frac{da}{dN}\right)_{l} = C_1a^{C_2};\quad a \geq d_2 \end{cases}, \tag{1}$$

where $A,\ B,\ C$ are materials constants, and d_1 and d_2 – microstructural barriers analytically determined after [4] as boundaries between the stages of SFC, PSFC and LFC, which practically stop crack propagation for some time. The values of the constants $A,\ B,\ C$ and the microstructural barriers d_1 and d_2 for the different steels are shown in Tables 3 and 4.

$\Delta\sigma$,	f,	Short Crack			Physically Small Crack			Long Crack	
MPa	*Hz*	A_1	A_2	A_3	B_1	B_2	B_3	C_1	C_2
ROLCLAS-09G2, Air									
387	**190**	–	–	–	-10.10^{-7}	$22{,}40.10^{-5}$	$-10{,}5.10^{-3}$	$24{,}8.10^{-7}$	1,7178
396		–	–	–	$-3{,}8.10^{-7}$	$9{,}97.10^{-5}$	$-4{,}74.10^{-3}$	$12{,}9.10^{-6}$	1,0484
405		–	–	–	–	–	–	$7{,}37.10^{-9}$	2,2138
RQT501*, 0.6M *NaCl									
516	**0.2**	-	-	-	$-3{,}9.10^{-7}$	$2{,}2.10^{-4}$	$-1{,}3.10^{-2}$	$1{,}7.10^{-6}$	1,7410
	0.5	$-3{,}9.10^{-6}$	$2{,}9.10^{-4}$	$-29{,}6.10^{-4}$	$-1{,}9.10^{-6}$	$4{,}6.10^{-4}$	-2.10^{-2}	$5{,}5.10^{-7}$	1,7355
	1	$-2{,}1.10^{-6}$	$2{,}1.10^{-4}$	$-1{,}1.10^{-4}$	$-1{,}4.10^{-6}$	$3{,}7.10^{-4}$	$-1{,}3.10^{-2}$	$6{,}6.10^{-7}$	1,6881
471	**0.2**	$-4{,}8.10^{-6}$	$5{,}39.10^{-4}$	-0,0139	$-3{,}2.10^{-6}$	$10{,}34.10^{-4}$	-0,05869	$1{,}43.10^{-7}$	1,9622
	0.5	$-6.4.10^{-7}$	-13.10^{-6}	0,0089	$-22,\ 9.10^{-7}$	$88{,}18.10^{-5}$	-0,06903	$8{,}34.10^{-7}$	1,6721
	1	$-2.9.10^{-6}$	$25{,}23.10^{-5}$	-0,00203	$-15{,}2.10^{-7}$	$50{,}8.10^{-5}$	-0,02565	$5{,}62.10^{-7}$	1,7115
396	**0.2**	$-3{,}28.10^{-6}$	$2{,}89.10^{-4}$	-0,00425	$-12{,}1.10^{-7}$	$3{,}46.10^{-4}$	-0,01782	$1{,}8.10^{-8}$	2,0787
	0.5	$-10{,}1.10^{-7}$	$33{,}41.10^{-6}$	0,00209	$-23{,}6.10^{-8}$	$13{,}36.10^{-5}$	-0,00591	$6{,}24.10^{-8}$	1,8943
	1	$-2{,}68.10^{-6}$	$31{,}56.10^{-5}$	-0,00132	$22{,}89.10^{-7}$	$36{,}40.10^{-5}$	-0,00972	$2{,}66.10^{-7}$	1,7304

Table 3. Characteristics of RQT501 and ROLCLAS-09G2 at different fatigue conditions

The graphical presentation of the model $da/dN - a$ from Eq. (1) can be seen in Fig. 3 for RQT501 and in Fig. 4 for ROLCLAS-09G2.

$\Delta\sigma$	f	d_1	d_2	$N_{f,exp}$	$N_{f,m}$	$100(N_{f,\exp} - N_{f,m})/N_{f,m}$
MPa	*Hz*	µm	µm	cycle	cycle	%
ROLCLAS-09G2, Air						
387	**190**	65	155	2120000	2236630	- 5,50
396		60	156	1690000	1778289	- 5,20
405		–	156	600000	634217	- 5,70
RQT501*, 0.6M *NaCl						
396	**0.2**	67	198.5	330269	299691	9.26
	0.5	60	155	223670	249228	- 11,43
	1	34	124	414000	405644	2,02
471	**0.2**	74	237	106800	104363	2.28
	0.5	108	268	109670	116949	- 6,64
	1	65	189	94900	93558	1,41
516	**0.2**	66	158	77389	73262	5.33
	0.5	63	163	132510	113399	14,42
	1	65	159	68550	79505	- 16,00

Table 4. Microstructural barriers and fatigue lifetimes of RQT501 and ROLCLAS-09G2

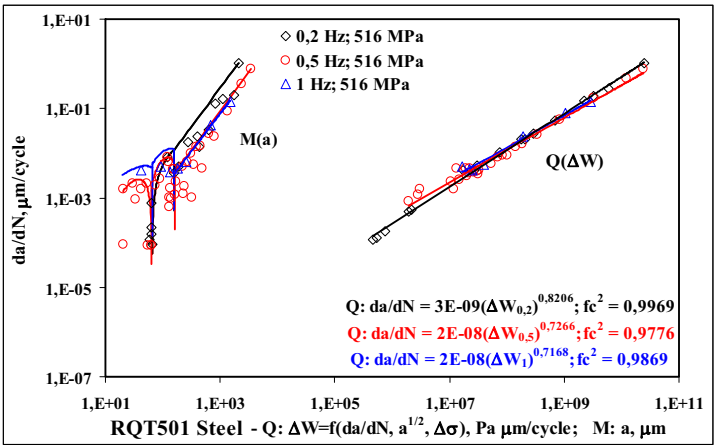

a.

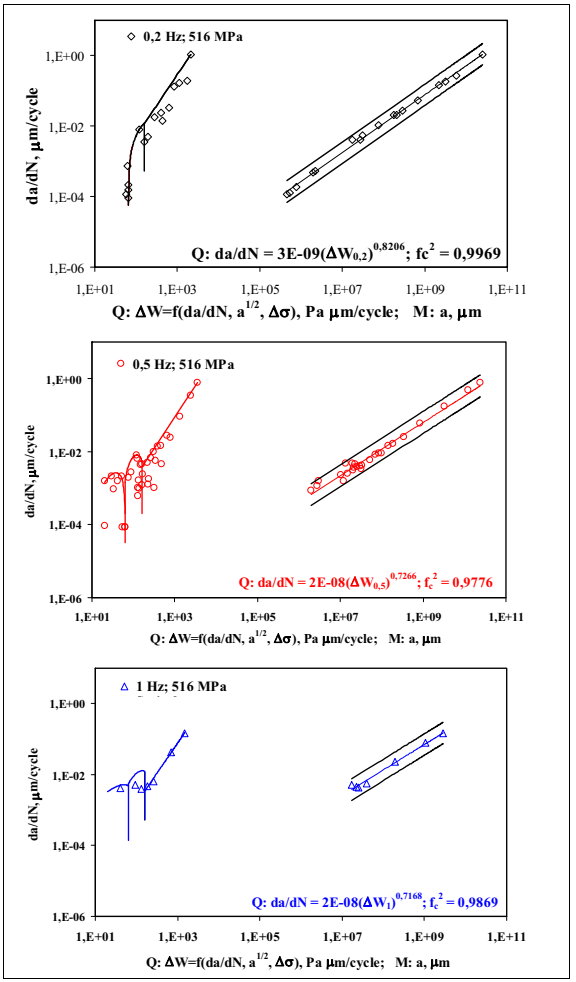

b.

Figure 3. Two models of the same fatigue data:

(*a*)

M(a) - Conventional three regime model;

Q(ΔW) - Alternative energy model

(*b*)

Models M(a) and Q(ΔW) at a single frequency

As illustrated in Figs. 3–4, a reasonable agreement can be seen when comparing experimental crack growth rates and theoretical crack growth rates obtained by the model of Eq. (1).

The proposed model is supported by the comparison of the fatigue lifetime predicted by Eq. (2), $N_{f,m}$, and the actual fatigue lifetime, $N_{f,\exp}$, both presented in Fig. 5:

$$N_{f,m} = N_{f0} + \int_{a_0}^{d_1} \frac{1}{L_{shc}\left(A_{shc}.a^2 + B_{shc}.a + C_{shc}\right)} da + \int_{d_1}^{d_2} \frac{1}{L_{psc}\left(A_{psc}.a^2 + B_{psc}.a + C_{psc}\right)} da + \int_{d_2}^{a_f} \frac{1}{L_{lc}A_{lc}.a^{B_{lc}}} da, \qquad (2)$$

where the coefficients *A, B, C, L* in $N_{f,\exp}$–expression are presented in Tabl. 4 and N_{f0} is the number of cycles of crack initiation.

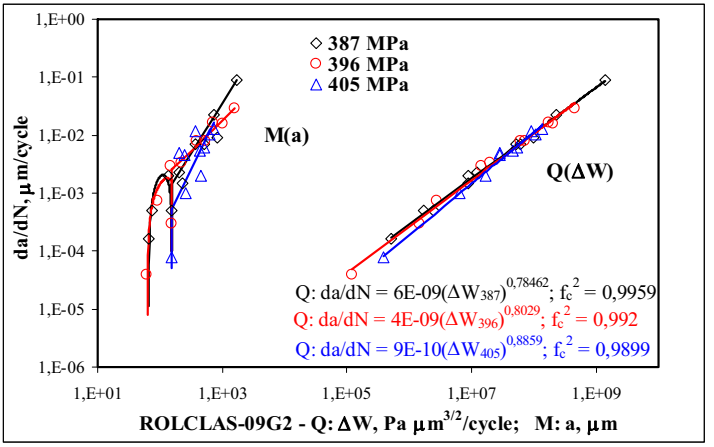

a.

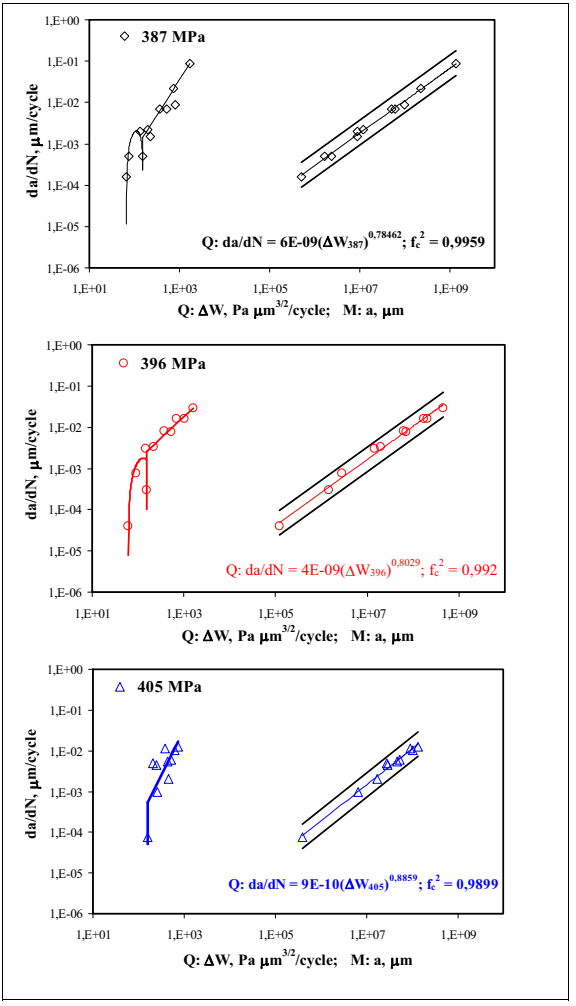

b.

Figure 4. Two models of the same fatigue data:

(a)

M(a) - Conventional three regime model;

Q(ΔW) - Alternative energy model;

(b)

Models M(a) and Q(ΔW) at a single stress range

In Figs. 3–***b*** and 4–***b*** scatter bands are indicated with two fine lines which correspond to the relations of a half and two folds in da/dN.

The results of fatigue lifetime $N_{f,m}$ predicted by Eq. (2) and presented in Table 4 and in Fig. 5 show that the model

$$da/dN = f(a)$$

from Eq. (1) gives a good fit expressed in maximum 16 %. for error bands around lifetime lines in Fig. 5.

At elastic-plastic conditions modelling is based on Eq. (3)

$$\log da/dN = C_J (\log \Delta J)^n \qquad (3)$$

(where C_J, n are scaling constants) and presented by a straight line as it can be shown in Hoshide [6, 7], and in Figs. 5 and 6. In Hoshide's publications there are some other presentations as well from the kind "Long or short fatigue crack growth rate, da_{sh}/dN or da_l/dN against J-integral range, ΔJ" on log-log scales, or $\log da_{sh}/dN - \log \Delta J$ and $\log da_l/dN - \log \Delta J$ which differ from lines.

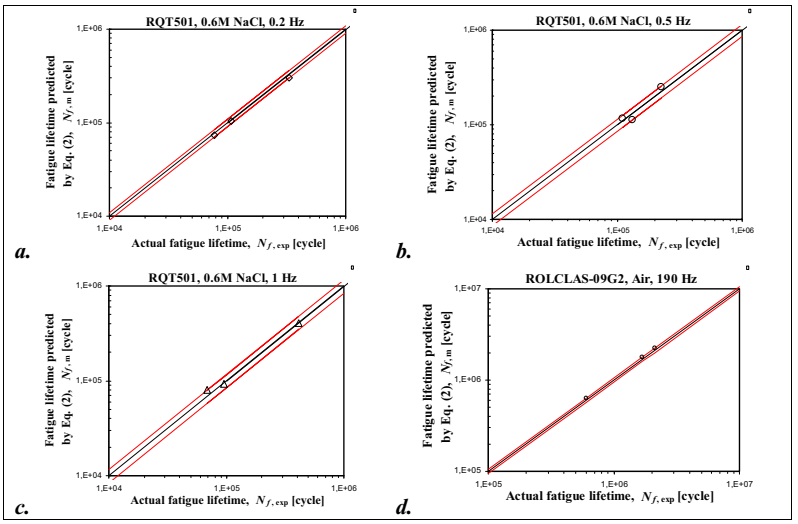

Figure 5. Steel fatigue lifetimes with their corresponding error bands for:

(*a*), (*b*), (*c*) RQT501

(*d*) ROLCLAS-09G2

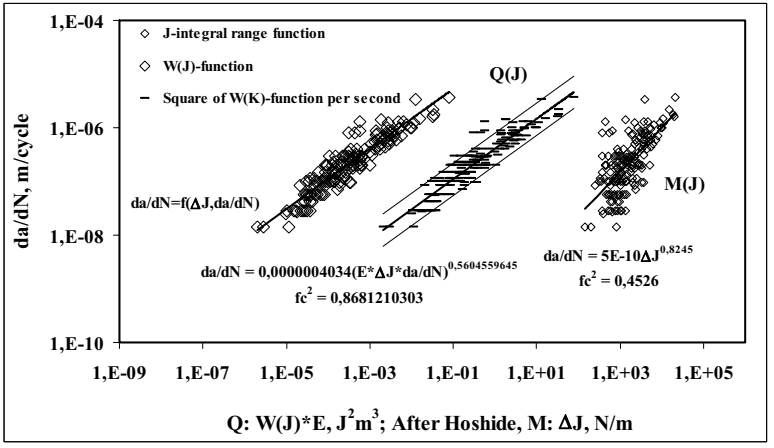

Figure 6. Two models of the same fatigue data for ($\alpha + \beta$) Ti alloy:

M(J) -Conventional three regime model;

Q(J) - Alternative energy model

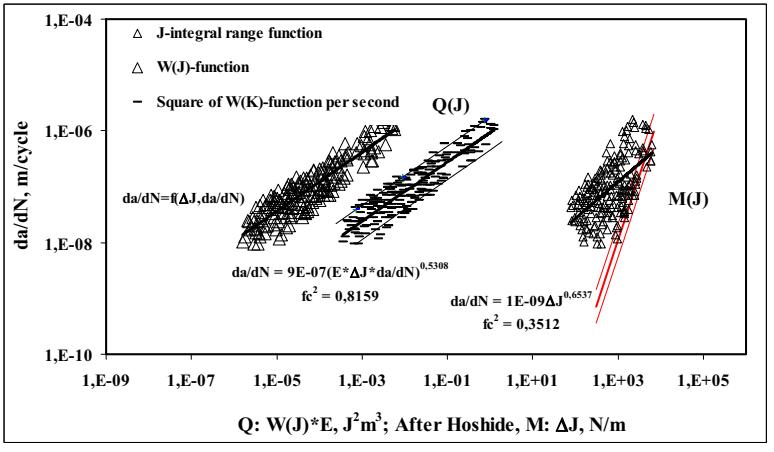

Figure 7. Two models of the same fatigue data for OFHC copper (the red line shows long crack data):

M(J) -Conventional three regime model;

Q(J) - Alternative energy model

An alternative method is proposed comprising fatigue testing of ingineering materials; measuring long-crack or main short-crack lengths a and the corresponding number of cycles N; calculating crack rates da/dN, stress-intensity factor range ΔK or short fatigue crack equivalent to it, $\Delta K_{sh} = k\sigma\sqrt{a_{sh}}$, or J-integral range ΔJ; and a newly introduced energy fatigue-function in its different versions — $W = (da/dN)\Delta K$ (or $kW = k(da/dN)\Delta K$), $W = (da/dN)\Delta J$, $W = (da/dN)a^{1/2}$, $W^* = f(ODA, N)$ — where k is a normalizing constant from the type $k = N_f / a_f K_{\max}(a_f)$, a_f and N_f are respectively the final length of fatigue crack and the number of cycles at failure, and $K_{\max}(a_f)$ is the stress intensity factor at $\sigma_{\max}$ from the applied stress range $\Delta\sigma = \sigma_{\max} - \sigma_{\min}$; kW is a non-dimensional expression. (The version $W^* = f(ODA, N)$ is described in detail in [11].) The physical sense of the fatigue function ΔW is that of a *specific* ***effective surface energy.*** The presentation $\log da/dN - \log W$ is an almost straight line Q(ΔW) or Q(J), shown as the thickest line in Figs. 3-4, 6-7, which may be termed "natural fatigue tendency" of material at a given stress range; this is mentioned for the first time in Angelova [10, 11, 12]. Each scatter band around such a line is indicated by two thin lines corresponding to ½ and 2 folds of *da/dN*. The alternative approach suggests a possible decrease of fatigue measurements and is approved for another 20 materials.

Summary
A conventional and an alternative approach to fatigue data presentations are compared for two steels and two non-ferrous alloys. The introduced energy fatigue function ΔW by the alternative approach transforms the presentations of crack-growth rate, da/dN against short crack length, a and J-integral range, ΔJ into a line $da/dN - \Delta W$. The line obtained may be termed *natural fatigue tendency* of material under a given stress range and because of its simplicity may be helpful for fatigue testing and practice in terms of precision and reduction of fatigue characterizing tests.

Acknowledgements. The authors thank Professor Toshihiko Hoshide, Kyoto University, Japan for the fatigue data of ΔJ investigations from [6, 7] and for the useful discussions about the specific experiments and the quantative evaluation of short fatigue crack growth based on EPFM analysis.
The authors thank MON and UCTM Bulgaria for the support on Contracts: TH-102; 10499; 10500.

References:

[1]. S. Suresh, *Fatigue of Materials*, Cambridge University Press, Cambridge, UK, (1998).

[2]. P.D. Hobson, M. Brown and E.R. de Los Rios, In: *ECF Publication 1. Mechanical Engineering Publications*, London, UK, (1986), pp. 441-459

[3]. D. Angelova and R. Akid, Fatigue Fract. Engng Mater. Struct. 21, (1998), pp. 771-779

[4]. R. Yordanova, *PhD Thesis,* University of Chemical Technology and Metallurgy, Sofia, (2003)

[5]. R. P. Gangloff, Res. Mechanica Letters, 1, (1981), pp. 299-306

[6]. T. Hoshide, T. Hirota and T. Inoue, Materials Sci. Research Int.,Vol. 1, No 3, (1995), pp. 169-174

[7]. T. Hoshide, T. Yamada, S.Fujimura and T.Hayashi, Eng. Frac. Mech., Vol. 21, No 1, pp. 85-101, (1985).

[8]. N. Dowling, *Mechanical Behaviour of Materials*, Prentice-Hall, New Jersey, USA, (2006).

[9]. Y.Murakami, *Metal Fatigue:Effects of Small Defects & Nonmetallic Inclusions*, Elsevier,Ox.,UK, (2002)

[10]. D.Angelova, In *ECF13 Proc.*, San Sebastian, Spain, Abstracts Vol., pp.128, Full text: ECF-CD, (2000)

[11]. D. Angelova, In *ECF16 Proc.*, Alexandroupolis, Greece, Full text: ECF-CD, (2006).

[12]. D. Angelova, In *Proceedings of IFMASS 8*, Belgrade, pp. 47-60, June 2003.